Synthesis of $Fe_4[Fe(CN)_6]_3 \cdot 14H_2O$ Nanopowder by Co-Precipitation Technique and Effect of Heat Treatment

S. Rohilla[a,b,*], B. Lal[c], S. Sunder[c], P. Aghamkar[c], S. Kumar[c] and A. Aggarwal[a]

[a]Materials Science Lab, Department of Applied Physics, Guru Jambheshwar University of Sc. & Tech., Hisar-125001, India

[b]The Technological Institute of Textile & Sciences, Bhiwani-127021, India

[c]Materials Science Lab, Department of Physics, Chaudhary Devi Lal University, Sirsa-125055, India

(Received March 5, 2010; in final form June 10, 2010)

Nanopowder of iron cyanide hydrate (member of Prussian blue family) was obtained using ferric chloride and potassium cyanide in their dilute solution through co-precipitation method. The effect of thermal annealing on iron cyanide hydrate nanocrystallites have been studied in detail. The formation of $Fe_4[Fe(CN)_6]_3 \cdot 14H_2O$ and iron oxides was revealed by the Fourier transform infrared spectroscopy. The crystal structure, morphology and size of nanocrystallites were investigated by X-ray diffraction and transmission electron microscope. Results suggest that using co-precipitation technique, nanopowder of iron cyanide hydrate, in typically spherical shape, can be obtained and their thermal treatment also yield iron oxide nanocrystallites of spherical with good homogeneity. The size of the prepared nanocrystallites was found in the range 20–36 nm. It was observed that thermal treatment, typically at 800 °C (4 h), iron cyanide hydrate ($Fe_4[Fe(CN)_6]_3 \cdot 14H_2O$) nanocrystallites transformed into iron oxide (α-Fe_2O_3, hematite) nanocrystallites.

PACS numbers: 81.07.−b, 64.70.Nd, 61.82.Rx

1. Introduction

The chemical and physical properties of inorganic compounds are fundamentally related to their chemical composition, size, shape, crystal structure and surface chemistry [1, 2]. Control of these factors allows one to observe unique properties of the materials. Amongst various inorganic compounds, Prussian blue (PB) [3, 4] is emerged as one of the most useful and promising compounds in the area of nanomagnetic devices [5], electrochemistry [6] and optics [7]. General formula of PB family is $A_n[B(CN)_6]_m \cdot xH_2O$, where A and B are transition metals. The magnetic properties, like saturation magnetization, transition temperature, coercive field etc., of this family can be manipulated by altering the concentration of magnetic ions [8] or by changing a magnetic ion by another magnetic ion [9, 10].

In the past, various forms of PB analogues were synthesized using different techniques such as [5, 8, 11, 12]. Among them, in solution technique the chances of getting contamination from outside are negligible. Therefore, in the present work, co-precipitation method is used to synthesize a PB analogue compound: iron cyanide hydrate ($Fe_4[Fe(CN)_6]_3 \cdot 14H_2O$). In addition, co-precipitation allows efficiently controlling the morphology and chemical composition of particles with good homogeneity. Kumar and Yusuf [12] reported the formation of polycrystalline ferriferricyanide ($Fe[Fe(CN)_6] \cdot xH_2O$) and investigated structural and magnetic properties of as-prepared sample. Interestingly, when we did the same experiment using piezoelectric nozzle method to form small droplets and control them at a higher temperature and change the concentration of the precursors used, large quantities of regular iron cyanide hydrate nanocrystals were obtained. Here it is worth mentioning that Kumar and Yusuf [12] used the simple pipette drop method for synthesizing the PB analogue. In simple pipette drop method it is difficult to control the size of droplets and dropping times. Also, it forms big droplets due to a big orifice diameter of pipette nozzle. Therefore, we used the piezoelectric nozzle method. In the piezoelectric nozzle process a solution is sprayed though a small orifice which is vibrated by a piezoelectric transducer. This method allows one to precisely control the droplet size and its dropping rate because wave of acoustic energy generates periodic instabilities that break the stream into a train of uniform droplets [13]. In the present article, synthesis of iron cyanide hydrate nanocrystallites, using co-precipitation technique, in powder form has been reported and the effect of heat treatment was studied. The samples were characterized by using complimentary techniques: Fourier transform infrared spectroscopy (FTIR), X-ray diffraction (XRD) and transmis-

* corresponding author; e-mail: rohillasunil2003@yahoo.co.in

sion electron microscopy (TEM). Results of as-prepared samples establish synthesis of fine and regular shape particles of iron cyanide hydrate having size in nanometer range with good homogeneity. A detailed study of effect of thermal treatment on iron cyanide hydrate nanocrystallites is made. At 800 ℃ (4 h) nanopowder of iron cyanide hydrate transforms into stable α-Fe_2O_3 (hematite) nanocrystallites.

2. Experimental

2.1. Sample preparation

The high purity reagents: potassium ferricyanide ($K_3[Fe(CN)_6]$); Aldrich 99.99%), ferric chloride ($FeCl_3$; Aldrich 99.99%), and de-ionized water were used. To prepare the sample 100 ml 0.08 M $K_3[Fe(CN)_6]$ aqueous solution was added through piezoelectric nozzle (nozzle size: 50 mm, 0.01 ml/s) to 200 ml 0.091 M $FeCl_3$ aqueous solution and the resulting solution was heated up to 80 ℃. The pH of the resultant solution was 11. To this end, hot solution was allowed to cool and further diluted to double of its initial volume. After cooling, dark bluish-green precipitates, so obtained, were filtered, washed many times with double distilled water and finally allowed to dry in air. The samples were grounded to very fine powder using pestle and mortar. The powder samples were sintered in muffle furnace (KSL 1600X, MTI) in air at different temperature and time duration, i.e. 600 ℃ (2 h), 700 ℃ (2 h) and 800 ℃ (4 h) using a ramp rate of 4 ℃/min.

2.2. Characterization

Complementary methods were used to characterize the structure and phase of as-prepared and sintered samples. Infrared spectra were collected by using the Fourier transform infrared spectrometer (Perkin Elmer 1600) ranging 4000–450 cm^{-1}. X-ray diffraction pattern of samples were carried out by a Philips X-ray diffractometer PW/1710; with Ni filter, using monochromatic Cu K_α radiation of wavelength 1.5418 Å at 50 kV and 40 mA. TEM of the samples was done with Philips EM400 electron microscope at an accelerating voltage of 100 kV.

3. Results and discussion

3.1. FTIR

The FTIR spectrum of the as-prepared sample is shown in Fig. 1a. In this spectrum, absorption band ranging from 3500 cm^{-1} to 2360 cm^{-1} is the characteristics of stretching vibration of OH which shows the presence of water in the sample. Further, the peak at 1602 cm^{-1} and 1414 cm^{-1} may be assigned to O–H banding mode [14]. The peak at 604 cm^{-1} and 449 cm^{-1} may be assigned to Fe–CN–Fe banding mode [15] and overlapping of v (Fe–C) and v (Fe–O) [16], respectively. The absorption band around 2080 cm^{-1} which is the strongest peak of FTIR spectrum shows the stretching mode of CN [17] for the PB-like compounds $[M^A_K[M_B(CN)_6]_L \cdot xH_2O$ $\{(K, L) = (1, 1)(4, 3)(3, 2)(2, 1)\}]$ in which cyanide forms bridges between M^A and M^B cations [18]. The presence of bluish green precipitate (on dissolving $K_3[Fe(CN)_6]$ with dilute mineral acid $FeCl_3$) along with 2080 cm^{-1} peak of FTIR spectrum confirms the formation of the iron cyanide hydrate.

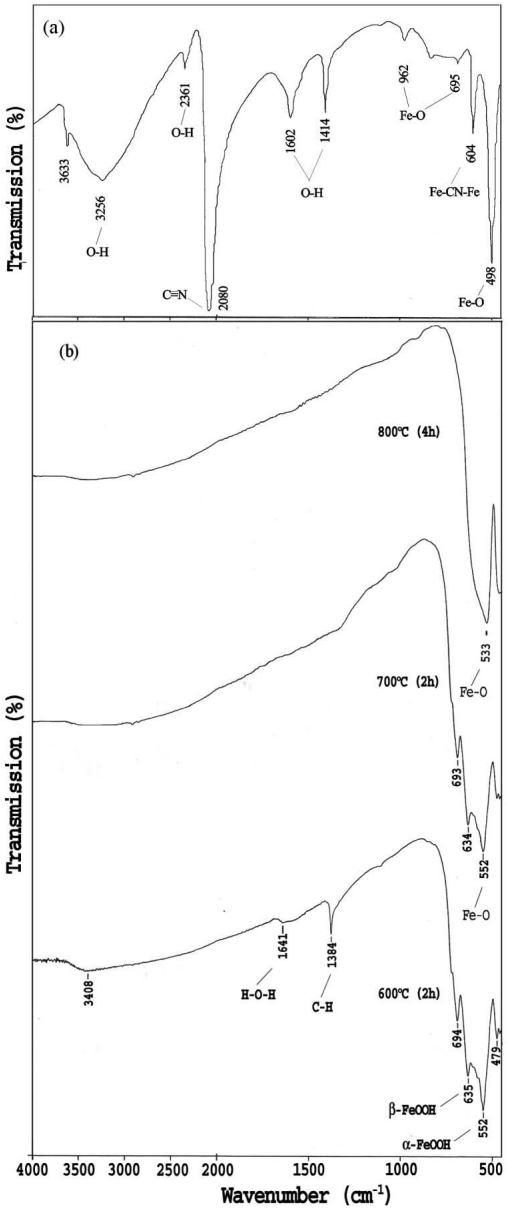

Fig. 1. (a) FTIR spectrum of as-prepared sample ($Fe_4[Fe(CN)_6]_3 \cdot 14H_2O$). (b) FTIR spectra of samples sintered at temperatures: 600 ℃ (2 h), 700 ℃ (2 h) and 800 ℃ (4 h).

Figure 1b shows transmission FTIR of the sample sintered at temperature 600 ℃ (2 h), 700 ℃ (2 h) and 800 ℃ (4 h) in the range 4000–450 cm^{-1}. At 600 ℃ (2 h) discrete medium peaks appeared between 475 and 695 cm^{-1}. In this low frequency region of FTIR spec-

trum, a medium peak appeared at 552 cm^{-1} and this is indicative peak of the Fe–O stretching vibration in iron oxide [16]. Besides, the peak centered about 479, 635 and 694 cm^{-1} may be assigned to hematite [19], α-FeOOH [20] and β-FeOOH [19, 20] phase, respectively. In addition, the peak centered at 1384 cm^{-1} can be ascribed to C–H bending vibration mode [21]. The weak band centered around 1641 cm^{-1} is due to the bending mode of H–O–H adsorbed at the Fe_3O_4 surface. The band centered at 3408 cm^{-1} may occur due to the overlapping of water band and surface hydroxyl group vibration [22]. When the sample was sintered at temperature 700 ℃ (2 h), the weak band at 1384 cm^{-1} and broad bands centered around 1641, 3408 cm^{-1} completely disappeared. The disappearance of these characteristic bands is due to elimination of volatiles hydrocarbon, water molecules and leads to densification of the nanopowder. At temperature 800 ℃ (4 h) the peaks of α-FeOOH and β--FeOOH completely disappeared and a new strong peak appeared at 533 cm^{-1} which is the characteristic peak of α-Fe_2O_3 [23]. This result indicates that the thermal annealing at temperature 800 ℃ (4 h) decomposes α-FeOOH and β-FeOOH into α-Fe_2O_3.

3.2. XRD

Figure 2a illustrates the crystal structure revealed by XRD pattern of the as-prepared sample. This figure shows a very strong diffraction peak at $2\theta \approx 17.5°$ (200), three peaks at 24.8° (220), 35.4° (400), 39.7° (420) and weak peaks at 50.8° (440) and 54.2° (600), which can be readily indexed to a face-centered-cubic phase (space group $Fm3m$) of iron cyanide hydrate with a lattice parameter of 10.28 Å [JCPDS file No. 73-0689]. These observations support the FTIR data. In order to obtain the average size of iron cyanide hydrate nanocrystallites, the well known Debye–Scherrer formula is employed and the size is found to be ≈ 22 nm.

Figure 2b shows the XRD data of the powder samples sintered in air at different temperature (600–800 ℃). The sample calcined at 600 ℃ (2 h) shows diffraction peaks centered around angle $2\theta \approx 30.2°$ (220), 35.6° (311), 57.5° (511) and 63.4° (440) which could be attributed to face-centered cubic Fe_3O_4 [JCPDS file no. 85-1436]. When the temperature was increased to 700 ℃ and clamped for 2 h, apparently no drastic change in the diffraction pattern was observed. However, when the diffraction pattern was minutely examined, we noticed that sharpness in the diffraction peak around $2\theta \approx 35.7°$ was increased but its intensity slightly reduced. The sharpness of the diffraction peak was expected because individual nanostructure merged together and as a result the activation energy becomes larger. In addition, a new but weak peak appeared around $2\theta \approx 33.1°$. This is indicative peak of α-Fe_2O_3. The average size of Fe_3O_4 and was found to be 25 nm and 28 nm for the sample sintered at 600 ℃ (2 h), 700 ℃ (2 h), respectively. This result shows that the crystallite size increases with increasing annealing temperature, which is well in agreement with reported results [24].

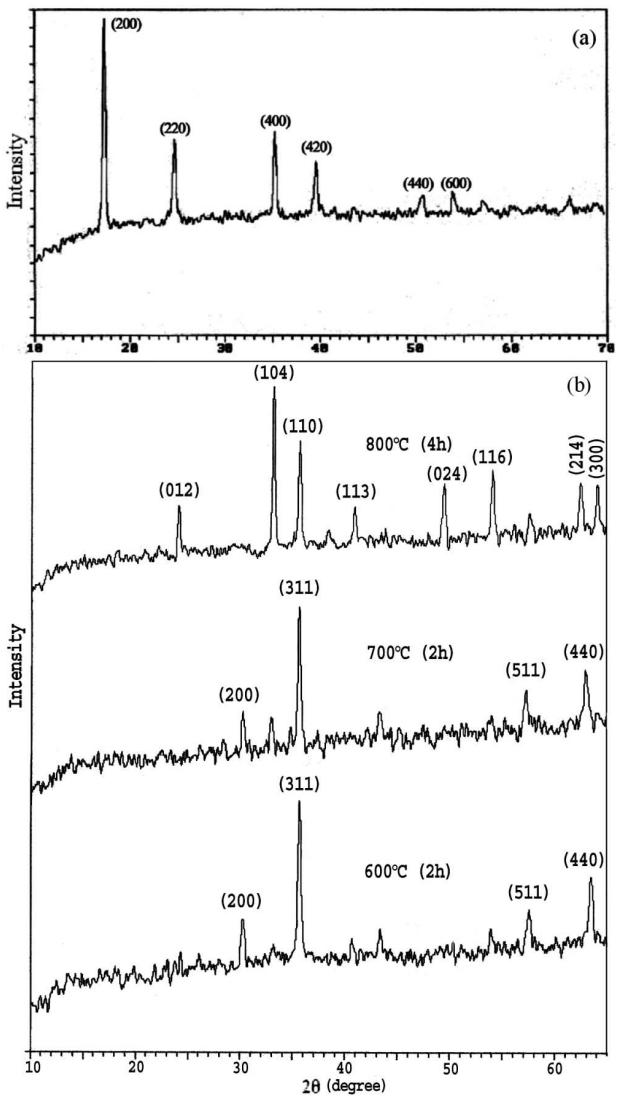

Fig. 2. (a) XRD pattern of as-prepared sample ($Fe_4[Fe(CN)_6]_3 \cdot 14H_2O$). (b) XRD pattern of the samples sintered at temperatures 600 ℃ (2 h), 700 ℃ (2 h) and 800 ℃ (4 h).

Finally, the sample was sintered at 800 ℃ (4 h) to study the effect of temperature and prolonged sintering time on structural changes of prepared sample. Interestingly, characteristic peaks of Fe_3O_4 disappeared while new peaks appeared around $2\theta \approx 24.1°$, 40.8°, 49.4°, 54° and 62.4°. In addition, strengthening of the characteristic peak ($2\theta \approx 33.1°$) of α-Fe_2O_3 was observed, which confirms the formation of most stable phase of iron oxide (α-Fe_2O_3). The diffraction peaks, centered at $2\theta \approx 24.1°$ (012), 33.1° (104), 35.6° (110), 40.8° (113), 49.3° (024), 54° (116), 62.4° (214) and 63.9° (300) may be assigned to hexagonal rhomb-centered α-Fe_2O_3 (hematite) [JCPDS File No. 72-0469]. This finding suggests that iron cyanide hydrate nanocrystallites can be transformed directly into stable α-Fe_2O_3 nanocrystallites by sintering at 800 ℃

(4 h) in air. The strong and sharp diffraction peak around $2\theta \approx 33.1^\circ$ was employed to estimate mean crystallite size of α-Fe_2O_3 and found to be ≈ 32 nm.

3.3. TEM

Figure 3a,b and c shows morphology of as-prepared and sintered samples at 600 ℃ (2 h) and 800 ℃ (4 h) as viewed under TEM. Micrograph 3a shows morphology

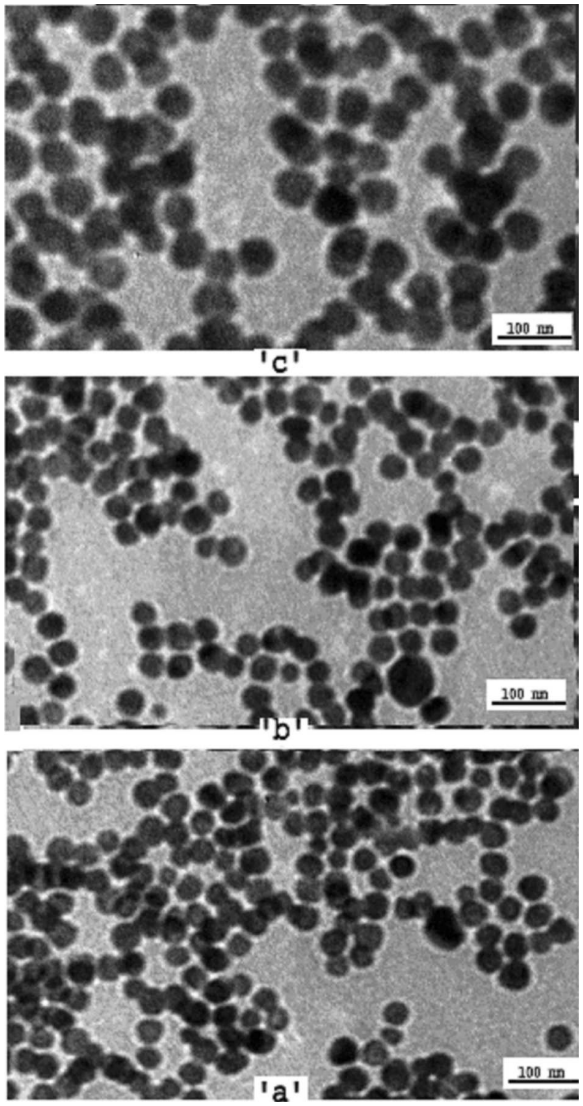

Fig. 3. TEM micrograph of the sample (a) as--prepared, (b) 600 ℃ (2 h) and (c) 800 ℃ (4 h).

of iron cyanide hydrate nanocrystallites i.e. as-prepared sample. It is clearly evident from micrograph that nanocrystallites are spherical in shape and weakly agglomerated. In addition, cluster appears pulpy with low density which may be due to presence of water molecules, hydrocarbon and volatile molecules. These observations support the XRD and FTIR data. Figure 3b and c clearly shows the influence of thermal annealing on as-prepared sample. The sintering eliminates water molecules, hydrocarbon and volatile molecules and as a result morphology, density, structure and size of nanocrystallites significantly modify. The size and density of nanocrystallites increase with rising sintering temperature due to coalescence of individual nanoparticles. As expected, the shape of nanocrystallites is spherical with good homogeneity and this may be due to technique used for the sample preparation [25].

4. Conclusions

The co-precipitation technique has been successfully used to prepare iron cyanide hydrate ($Fe_4[Fe(CN)_6]_3 \cdot 14H_2O$), nanocrystallites having size 22–40 nm. Upon thermal treatment at 600 ℃ (2 h) and 800 ℃ (4 h) in air, Fe_3O_4 (24 nm) and α-Fe_2O_3 (32 nm) nanocrystallites were obtained. The crystal structure, structural change and morphology of nanocrystallites were investigated by FTIR, XRD and TEM. The results of FTIR are well in agreement with available data. Results of XRD and TEM support the FTIR data as well as are compatible with each other. The present studies also suggest that iron cyanide hydrate nanocrystallites can be transformed into iron oxide (α-Fe_2O_3) nanocrystallites at 800 ℃ (4 h), which have many potential applications such as magnetic storage media, catalyst, magnetic and optical properties, environment protection, sensors, clinical diagnosis, etc. In addition, the present work establishes co-precipitation technique with spraying of drops (through piezoelectric process) whose arrangement is successful wet chemical method to synthesize fine and uniform particle size with non-agglomerate particles, easily scale-up, low cost and time saving technique. Moreover, shape of the nanocrystallites (PB family and iron oxide) are spherical with uniform homogeneity as compared to earlier reports [12, 26, 27]. Here it is worth pointing out that PB suspension can be mixed with the other metal oxide, e.g. SiO_2 or polymer to prepare nanocomposites. This would be a matter of future communications.

Acknowledgments

Authors thankfully acknowledge DST (FIST), New Delhi for financial assistance.

References

[1] A.P. Alivisatos, *Science* **271**, 933 (1996).

[2] C. Burda, X. Chen, R. Narayanan, M.A. El-Sayed, *Chem. Rev.* **105**, 1025 (2005).

[3] A. Goux, J. Ghanbaja, A. Walcarius, *J. Mater. Sci.* **44**, 6601 (2009).

[4] M. Verdaguer, A. Bleuzen, V. Marvaud, J. Vaissermann, M. Seuleiman, C. Desplanches, A. Scuiller, C. Train, R. Garde, G. Gelly, C. Lomenech, I. Rosenman, P. Veillet, C. Cartier, F. Villain, *Coord. Chem. Rev.* **190-192**, 1023 (1999).

[5] L. Catala, A. Gloter, O. Stephan, G. Rogez, T. Mallaha, *Chem. Commun.*, 1018 (2006).

[6] K.R. Dunbar, R.A. Heintz, *Prog. Inorg. Chem.* **45**, 283 (1997).

[7] J.G. Moore, E.J. Lochner, C. Ramsey, N.S. Dalal, A.E. Stiegman, *Angew. Chem., Int. Ed.* **42**, 2741 (2003).

[8] S. Ohkoshi, T. Iyoda, A. Fujishima, K. Hashimoto, *Phys. Rev. B* **56**, 11642 (1997).

[9] S. Ferlay, T. Mallah, R. Quahés, P. Veillet, M. Verdaguer, *Nature* **378**, 701 (1995).

[10] V. Gadet, T. Mallah, I. Castro, M. Verdaguer, P. Veille, *J. Am. Chem. Soc.* **114**, 9213 (1992).

[11] T. Uemura, S. Kitagawa, *J. Am. Chem. Soc.* **125**, 7814 (2003).

[12] A. Kumar, S.M. Yusuf, *Pramana J. Phys.* **63**, 239 (2004).

[13] D.K. Kim, Y. Zhang, W. Voit, K.V. Rao, M. Muhammed, *J. Magn. Magn. Mater.* **225**, 30 (2001).

[14] R. Balasubramaniam, A.V. Ramesh Kumar, *Corrosion Sci.* **42**, 2085 (2000).

[15] *IR Spectra of Inorganic Compounds*, Eds. R.A. Nyquist, R.A. Kagel, Academic Press, New York 1971.

[16] R. Balasubramaniam, A.V. Ramesh Kumar, P. Dillman, *Current Sci.* **85**, 1546 (2003).

[17] Ji B. Ayers, W.H. Waggoner, *J. Inorg. Nucl. Chem.* **33**, 721 (1971).

[18] A. Ludi, H.U. Gudel, *Struct. Bond.* **14**, 11 (1973).

[19] A. Saric, S. Music, K. Nomura, S. Popovic, *Croatica Chem. Acta* **71**, 1019 (1998).

[20] A. Bertoluzza, C. Fagnano, M.A. Morelli, V. Gottardi, M. Guglielnie, *J. Non-Cryst. Solids* **48**, 117 (1982).

[21] P.D. Maniar, A. Navrotsky, E.M. Rabinovich, J.Y. Ying, J.B. Benziger, *J. Non-Cryst. Solids* **124**, 101 (1990).

[22] S.P. Castaneda, J.R. Martinez, F. Ruiz, S.P. Sanchez, O. Dominguez, *J. Solgel Sci. Technol.* **25**, 29 (2002).

[23] F.F. Bentley, L.D. Simthson, A.L. Rozek, *Infrared Spectra and Characteristic Frequencies*, Inter Sci. Publ., New York 1968.

[24] V.T. Liveri, *Controlled Synthesis of Nanoparticles in Microheterogeneous Systems*, Springer, Berlin 2006.

[25] Y.F. Chen, S.R. Sheen, *J. Chin. Chem. Soc.* **47**, 307 (2000).

[26] V. Vo, M.N. Van, H.I. Lee, J.M. Kim, Y. Kim, S.J. Kim, *Mater. Chem. Phys.* **107**, 6 (2008).

[27] Y. Nuli, R. Zeng, P. Zhang, Z. Guo, H. Liu, *J. Power Sources* **184**, 456 (2008).